Inter*net* Electronic Journal of Molecular Design

April 2003, Volume 2, Number 4, Pages 242–261

Editor: Ovidiu Ivanciuc

Special issue dedicated to Professor Haruo Hosoya on the occasion of the 65th birthday
Part 8

Guest Editor: Jun–ichi Aihara

3D–QSAR of Cyclooxygenase–2 Inhibitors by Genetic Function Approximation

Anand V. Raichurkar and Vithal M. Kulkarni

Pharmaceutical Division, Institute of Chemical Technology, University of Mumbai, Mumbai 400019, India

Received: October 23, 2002; Revised: January 28, 2003; Accepted: February 7, 2003; Published: April 30, 2003

Citation of the article:
A. V. Raichurkar and V. M. Kulkarni, 3D–QSAR of Cyclooxygenase–2 Inhibitors by Genetic Function Approximation, *Internet Electron. J. Mol. Des.* **2003**, *2*, 242–261, http://www.biochempress.com.

Copyright © 2003 **BioChem** Press

Inter*net* Electronic Journal of Molecular Design

BioChem Press
http://www.biochempress.com

3D–QSAR of Cyclooxygenase–2 Inhibitors by Genetic Function Approximation[#]

Anand V. Raichurkar and Vithal M. Kulkarni*

Pharmaceutical Division, Institute of Chemical Technology, University of Mumbai, Mumbai 400019, India

Received: October 23, 2002; Revised: January 28, 2003; Accepted: February 7, 2003; Published: April 30, 2003

Internet Electron. J. Mol. Des. **2003**, *2* (4), 242–261

Abstract

The invention of selective cyclooxygenase–2 (COX–2) inhibitors peaks the first phase of an exciting and fast paced effort to exploit a novel target for nonsteroidal anti–inflammatory drugs (NSAIDs). A series of molecules has been reported as specific COX–2 inhibitors belonging to the class of tetrahydroisoindole nucleus. A 1,3–diaryl substitution on the central polycyclic ring system and absence of sulfonyl moiety are the two structural features of this chemical series. We report the three–dimensional quantitative structure–activity relationship (3D–QSAR) performed by genetic function approximation (GFA) on this class of compounds. QSAR models were generated using a training set of 20 compounds and the predictive ability of each model was assessed using a set of 7 molecules. The internal and external consistency of the final QSAR model was 0.656 and 0.669 respectively. The results indicate that shape (steric), electronic and spatial (conformational) descriptors govern the COX–2 enzyme inhibition. The descriptors appeared in the final model are compatible with the COX–2 enzyme topology. A hypothetical mechanism of enzyme–inhibitor interaction was derived to gain important structural insights into designing novel antiinflammatory agents prior to their synthesis.

Keywords. Three–dimensional quantitative structure–activity relationships; 3D–QSAR; genetic function approximation; GFA; NSAIDs; cyclooxygenase–2; COX–2 inhibitors; tetrahydroisoindoles.

1 INTRODUCTION

The history of non–steroidal antiinflammatory drugs (NSAIDs), which are used for the treatment of pain, inflammation and fever, is rich and well documented. The discovery in 1971 by Vane, that cyclooxygenase (COX) is their molecular target was a landmark finding but did not reasoned the undesired effects such as gastric irritation of classical NSAIDs [1]. It was postulated recently that an inflammatory or mitogenic stimulus might result in gene expression responsible for the synthesis of a second, inducible COX isoenzyme called COX–2, which is very similar in structure to its constitutive counterpart COX–1 and its inhibition itself is sufficient to produce desired antiinflammatory effect without any side effects [2]. This hypothesis gave an opportunity to

[#] Dedicated to Professor Haruo Hosoya on the occasion of the 65th birthday.

* Correspondence author; phone: +91–22–24145616; fax: +91–22–24145614; E–mail: vithal@biogate.com.

differentiate desired and undesired effects of COX isoforms in the treatment of inflammation with classical NSAIDs. The importance of the COX–2 discovery is reflected in the unprecedented speed at which different research laboratories developed extensive libraries of selective COX–2 enzyme inhibitors as a new class of antiinflammatory, analgesic and antipyretic drugs with significantly reduced side effects. Recent epidemiological and experimental data suggest that selective inhibition of COX–2 could also be an important strategy for preventing or treating number of diseases such as cancer, Alzheimer's, cardiovascular (angiogenesis) and blood clotting disorders [3]. Hence, there is a need to develop more selective COX–2 enzyme inhibitors with broad range of activities without any side effects.

The recent invention of selective COX–2 inhibitors: celecoxib, rofecoxib and valdecoxib climaxes the first phase of a fast paced effort to exploit novel target for NSAIDs. The COX–2 inhibitors belonging to a tricyclic group of compounds possess a diarylstilbene core with a sulfonyl ($–SO_2–$) group at para position on one of the aromatic rings [4] (Figure 1).

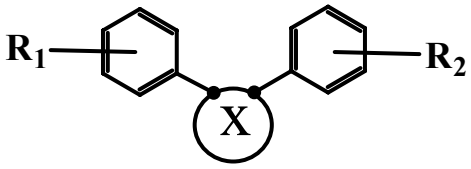

Figure 1. General structure of selective tricyclic COX–2 inhibitors.

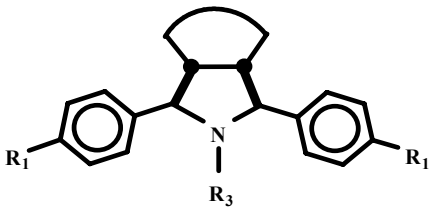

Figure 2. General structure of selective new isoindole derivatives.

New COX–2 inhibitors continue to emerge from the patent literature. Many are variation of tricyclic or classical NSAIDs. Recently, Guillaume *et al*. reported a diverse series of molecules, belonging to the class of tetrahydroisoindoles as COX–2 enzyme inhibitors with potent antiinflammatory activity and reduced side effects [5] (Figure 2). The series stand out as a new class among the COX–2 inhibitors reported till date and is characterized by the absence of diarylstilbene core and sulfonyl ($–SO_2–$) group on aromatic ring, which are considered to induce selectivity for tricyclic compounds. This series is evident for the flexibility of the COX–2 active site [6]. This stimulated to study further and understand the factors responsible for therapeutic activity or inhibitory potency for such diverse molecules inhibiting COX–2 enzyme.

Though the crystal structure of ovine COX–1, murine COX–2, and human COX–2 enzymes with or without ligands are solved, the *de novo* design or optimization of COX–2 selectivity of inhibitors is not an easy task, due to (*a*) the physicochemical and kinetic factors hidden in X–ray crystal structure could be involved in the inhibition and (*b*) the flexibility of the COX–2 active site [6]. In such cases generating 3D–QSAR models using various physicochemical descriptors can yield information to understand the factors responsible for biological activity. Our strategy follows the methodology used previously to generate successful 3D–QSAR models for antifungal, antibacterial,

antiHIV–1, antidiabetic, and antitubercular agents [7–11].

In order to deduce the correlation between structural and biological activity of present series of molecules, Genetic Function Approximation (GFA) has been used to generate different 3D–QSAR models from various descriptors available within Cerius2 molecular modeling software [12]. GFA generates a population of equations for correlation between biological activity and physico–chemical properties. GFA developed by Rogers involves combination of Friedman's multivariate adaptive regression splines (MARS) algorithm with Holland's genetic algorithm to evolve a population of equations that best fit the training set data [12–17]. This is done as follows: (*a*) An initial population of equations is generated by random choice of descriptors. The fitness of each equation is scored by lack–of–fit (LOF) measure, $LOF = LSE/\{1 - (c + d \times p)/m\}^2$, where LSE is the least square error, c is the number of basis functions in the models, d is the smoothing parameter which controls the number of terms in the equation, p is the number of features contained in all terms of the models, and m is the number of compounds in the training set. (*b*) Pairs from the population of equations are chosen at random and 'crossovers' are performed and progeny equations are generated. (*c*) The fitness of each progeny equation is assessed by LOF measure. (*d*) If the fitness of new progeny equation is better, then it is preserved. The model with proper balance of all statistical terms will be used to explain the variance in the biological activity.

A distinctive feature of GFA is that instead of generating a single model, as do most other statistical methods, it produces a population of models (*e.g.*, 100). The range of variation in this population gives added information on the quality fit and importance of descriptors. By examining these models, additional information can be obtained. For example, the frequency of use of a particular descriptor in the population of equations may indicate how relevant the descriptor is to the prediction of activity. Combination of robust statistical technique GFA coupled with the use of different types of descriptors would result in better prediction of biological activity for COX–2 enzyme inhibitors as antiinflammatory agents. In this paper, we present 3D–QSAR models for the 1,3–diaryltetrahydroisoindoles as COX–2 inhibitors with antiinflammatory activity.

2 MATERIALS AND METHODS

2.1 Chemical Data

2.1.1 Molecules

In the present study a set of 27 molecules belonging to 1,3–diaryltetrahydroisoindoles as COX–2 inhibitors with antiinflammatory activity were taken from the literature and used [5]. A training set containing 20 molecules (Table 1) was used for the generation of QSAR models. A test set of 7 molecules (Table 2) with uniformly distributed biological activities was used to test the predictive ability of the generated models.

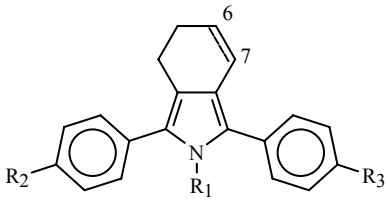

Compounds **1**–**9**

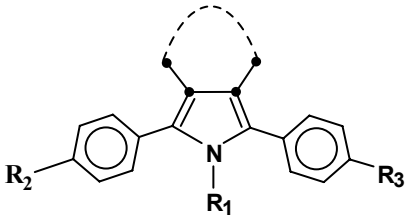

Compounds **13**–**27**

Table 1. Structures and biological activities of the molecules from the training set

No	Structure	Ring	R_1	R_2	R_3	IC_{50} COX–2	IC_{50} COX–1
1	–	–	H	H	H	1.5	100
2 [a]	–	–	H	H	H	3.3	100
3	–	–	NH_2	H	H	1.8	1000
4	–	–	$NHSO_2CH_3$	H	H	500	>1000
5	–	–	H	F	F	1.7	100
6	–	–	H	CH_3	CH_3	16.7	500
7	–	–	H	OCH_3	OCH_3	21.3	1000
8	–	–	H	Cl	Cl	5	>5000
9	–	–	H	F	imidazolyl–1–yl	42	500
10	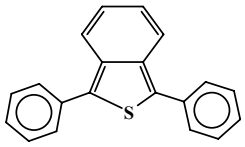	–	–	–	–	10.9	1000
11	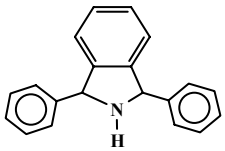	–	–	–	–	32.4	>2500
12	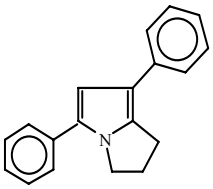	–	–	–	–	50.0	<1000
13	–		H	H	H	3.1	1000
14	–		H	H	H	14.5	>100
15	–		H	H	H	0.7	250
16	–		H	F	F	2.9	100
17	–		H	H	H	2.6	100
18	–		H	F	SO_2CH_3	700	>5000
19	–		H	F	F	4.5	500
20	–		H	F	F	0.6	230

[a] double bond present between positions 6 and 7

Table 2. Structures and biological activities of test set compounds

No	Structure	Ring	R_1	R_2	R_3	IC_{50} COX–2	IC_{50} COX–1
21	–		H	SCH_3	SCH_3	500	500
22	–		H	F	F	1.1	100
23	–		H	H	H	1.6	250
24	–		H	H	H	35.6	>5000
25	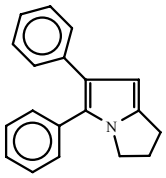	–	–	–	–	10	<1000
26	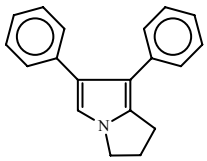	–	–	–	–	28.7	2500
27	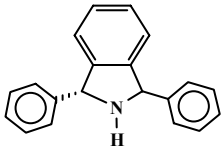	–	–	–	–	10	>2500

2.1.2 Biological activity

Biological activities of the molecules in terms of pIC_{50} (IC_{50} = log $1/IC_{50}$) values of concentrations in unit of μM required for 50% of inhibition against COX–2 enzyme isolated from mouse resident peritoneal macrophages, were used in the present study. Further details of the biological testing can be found in [5].

2.2 Molecular Modeling

2.2.1 Software

All molecular modeling studies were carried out using Cerius2 (version 3.5) running on Silicon Graphics O2 R5000 workstation [18]. Structures were constructed and partial charges were assigned using the charge equilibration method within Cerius2 [19]. Throughout the study, the Universal forcefield 1.02 was used. The molecules were subsequently minimized until a root mean square deviation 0.001 kcal/mol Å was achieved and used in the study.

2.2.2 Calculation of descriptors

Different types of descriptors were calculated for each molecule in the study table using default settings within Cerius2. These descriptors included electronic, spatial, structural, thermodynamic,

and molecular shape analysis (MSA). A complete list of descriptors used in the study is given in Table 3.

Table 3. Descriptors used in the present study

No	Descriptor	Type	Description
1	Vm	Spatial	Molecular volume [d]
2	Area	Spatial	Molecular surface area [d]
3	Density	Spatial	Molecular density [d]
4	RadOfGyration	Spatial	Radius of gyration [d]
5	PMI–mag	Spatial	Principle moment of inertia [d]
6	PMI–X	Spatial	Principle moment of inertia X–component
7	PMI–Y	Spatial	Principle moment of inertia Y–component
8	PMI–Z	Spatial	Principle moment of inertia Z–component
9	MW	Structural	Molecular weight [d]
10	Rotlbonds	Structural	Number of rotatable bonds [d]
11	Hbond acceptor	Structural	Number of hydrogen bond acceptors [d]
12	Hbond donor	Structural	Number of hydrogen bond donors [d]
13	AlogP	Thermodynamic	Logarithm of partition coefficient [d]
14	MolRef	Thermodynamic	Molar refractivity [d]
15	Dipole–mag	Electronic	Diploe moment [d]
16	Dipole–X	Electronic	Diploe moment–X–component
17	Dipole–Y	Electronic	Dipole moment–Y–component
18	Dipole–Z	Electronic	Dipole moment–Z–component
19	Charge	Electronic	Sum of partial charges [d]
20	Apol	Electronic	Sum of atomic polarizabilities [d]
21	HOMO	Electronic	Highest occupied molecular orbital energy
22	LUMO	Electronic	Lowest unoccupied molecular orbital energy
23	Sr	Electronic	Superdelocalizability
24	Foct	Thermodynamic	Desolvation free energy for octanol
25	Fh_2o	Thermodynamic	Desolvation free energy for water
26	Hf	Thermodynamic	Heat of formation
27	DIFFV	MSA	Difference volume
28	COSV	MSA	Common overlap steric volume
29	Fo	MSA	Common overlap volume ratio
30	NCOSV	MSA	Non–common overlap steric volume
31	Shape RMS	MSA	RMS to shape reference
32	SR Vol	MSA	Volume of shape reference compound

[d] default descriptor

2.2.3 MSA descriptors

MSA descriptors were calculated using MSA module within Cerius2 [20]. Conformational analyses on all the molecules were performed using random sampling search with maximum number of conformers set to 50. Lowest energy conformer of the most active molecule was used as reference for calculation of MSA descriptors.

2.2.4 Generation of QSAR models

QSAR analysis is an area of computational research, which builds models of biological activity using physico–chemical properties of a series of compounds. The underlying assumption is that the variations of biological activity within a series can be correlated with changes in measured or computed molecular features of the molecules. In the present study, QSAR model generation was

performed by GFA technique. The application of the GFA algorithm allows the construction of high–quality predictive models and makes available additional information not provided by standard regression techniques, even for data sets with many features. GFA was performed by using 20,000 crossovers, a smoothness value of 1.00 and other default settings for each combination. The number of terms in the equation was fixed to 4 including the constant in the training set. The equations generated were evaluated on the following basis: (*a*) LOF measure; (*b*) Variable terms in the equation; (*c*) Internal and external predictive ability of the equation.

The predictive r^2 was based only on molecules not included in the training set and is defined as: r^2_{pred} = (SD – PRESS)/SD, where SD is the sum of the squared deviations between the biological activity of molecules in the test set and the mean biological activity of the training set molecules and PRESS is the sum of the squared deviations between predicted and actual activity values for every molecule in the test. Like $r^2_{cv,}$ the predictive r^2 can assume a negative value reflecting a complete lack of predictive ability of the training set for the molecules included in the test set [21,22].

3 RESULTS AND DISCUSSION

3.1 Results

In the present study only those molecules were used for which absolute IC_{50} values were available and thus QSAR models were generated using a training set of 20 molecules. Test set of 7 molecules with regularly distributed biological activities was used to assess the predictive power of generated QSAR models. Biological activity was expressed in terms of log $1/IC_{50}$ (μm) against COX–2 enzyme. The conformational space of the rotatable bonds in the molecule was explored using random sampling technique in order to obtain sterically accessible conformations within optimum computational time. Conformational search using random sampling was performed, during the MSA technique; the lowest energy conformers were selected for alignment. All the molecules were aligned on lowest energy conformer of the most active molecule (compound **20**). GFA was used for generation of QSAR models with 20,000 crossovers and the smoothness value *d* of 1.0.

3.1.1 Significance of molecular descriptors

The Cerius2 QSAR generates different descriptors belonging to different categories like conformational, electronic, shape, spatial, thermodynamic, *etc*. Interpretation of QSAR models with more terms becomes difficult for drug design. Moreover all the terms may not be relevant. To obtain stable and consistent results from GFA and also to determine relevant descriptors, we used a procedure to select a subset of descriptors, from a much large pool of descriptor. GFA was run

several times by using molecular descriptors in several combinations to generate different QSAR models containing not more than four terms per equation.

Four models were generated using combination of different descriptors: Model A: Using default descriptors; Model B: Default + Thermodynamic descriptors; Model C: Default + MSA descriptors; Model D: Combination of all descriptors. All the statistically significant equations for each QSAR model are given in Table 4. The term BA in these equations represents biological activity expressed as pIC_{50} values.

Table 4. Summary of the best equation selected from different GFA models. Model D is selected to explain the observed antiinflammatory activity of tetrahydroisoindole derivatives

No	Equation	LOF	r^2	r^2_{cv}	F–value	r^2_{pred}	Parameter
Model A	BA = 2.417590 + 0.833226 AlogP – 0.000346 Apol + 0.524673 Hbond donor – 0.185838 RadOfGyration	0.546	0.709	0.510	9.14	0.735	Default
Model B	BA = 1.963100+ 0.833146 AlogP – 0.000371 Apol + 0.530211 Hbond donor	0.405	0.706	0.539	12.81	0.711	Default Thermodynamic
Model C	BA = 2.663920 + 0.008006 COSV + 0.700323 AlogP – 0.000458 Apol	0.401	0.709	0.524	13.01	0.705	Default MSA
Model D	BA = 1.476940 + 0.013920 COSV + 0.561998 Dipol–Z – 0.000360 PMI–Z	0.313	0.773	0.656	18.18	0.669	All

Model A. QSAR equations using GFA were generated using default descriptors. The resultant equations were evaluated for their predictive power. As evident from the variable usage graph, molecular descriptors: AlogP, Hbond donor, Rotlbonds and Apol were frequently used in the generation of QSAR models. A single best equation from the set of equations was selected on the basis of good internal and external predictivity, variable terms, LOF value, and other statistical terms like higher F value. The variable terms in the equation show low correlation among themselves indicating less probability of chance correlation.

Model B. This model was built by combination of default and thermodynamic descriptors. The resultant set of equations were evaluated on the basis of cross–validated r^2 (r^2_{cv}), non–cross validated r^2, LOF, variable terms. As indicated by variable usage graph the generations of set of equations were dominated by repeated use of AlogP, Vm, MolRef and Apol. The single best equation was chosen having highest external predictive power. Addition of thermodynamic descriptor to QSAR table increased the internal predictivity moderately but has low LOF and higher F value than the model generated by using default descriptors.

Model C. Deviation in the biological activity for a series of molecules can be explained on the basis of differences in the physico–chemical descriptors. Hence, we considered the use of shape related descriptors in the generation of QSAR models. Six MSA descriptors were calculated using MSA module added to QSAR table and Model C was generated. The equations were analyzed on the basis of important statistical parameters used in the earlier models. Descriptors like NCOSV, AlogP, Hbond acceptor, COSV, and Apol were repeatedly used to generate QSAR Model C. A single best equation was selected with proper balance of statistical terms. The internal predictivity

of equation is more than Model A and slightly less than Model B, where as the external predictivity is comparable as that of both Model A and B. The equation also has low LOF and higher F value than Model A and B. Therefore the equation clearly shows the importance of shape related descriptors.

Table 5. Summary of the five best GFA equations of Model D. Eq. (3) is the representative equation of Model D

No	Equation	LOF	r^2	r^2_{cv}	F–value	r^2_{pred}
1	BA = 0.755642 – 0. 001976 PMI–mag + 0.483868 Dipol–Z + 3.980070 Fo	0.307	0.777	0.678	18.588	0.654
2	BA = 0.735826. – 0.002652 PMI–Z + 0.475220 Dipol–Z + 4.084670 Fo	0.311	0.774	0.673	18.278	0.642
3	BA = 1.476940 + 0.013920 COSV + 0.561998 Dipol–Z – 0.000360 PMI–Z	0.313	0.773	0.656	18.180	0.669
4	BA = 1.663190 + 0.872127 AlogP – 0.181546 Foct – 0.028770 Vm	0.373	0.729	0.574	14.383	0.623
5	BA = 3.377270 + 0.647270 AlogP – 0.010086 NCOSV – 0.000306 Apol	0.378	0.726	0.541	14.122	0.662

Table 6. Observed and predicted biological activities of training set of molecules. Results computed with Model D, Table 4

Molecule	Observed pIC_{50}	Calculated pIC_{50}	Residual
1	2.830	1.874	0.956
2	2.481	2.492	–0.011
3	2.744	2.482	0.262
4	0.301	0.834	–0.533
5	2.769	2.843	–0.074
6	1.777	1.962	–0.185
7	1.672	1.470	0.201
8	2.301	2.204	0.092
9	1.377	0.987	0.390
10	1.962	2.658	–0.696
11	1.489	1.630	–0.141
12	1.301	1.909	–0.608
13	2.509	2.408	0.101
14	1.839	2.101	–0.263
15	3.154	2.441	0.713
16	2.537	2.645	–0.108
17	2.585	2.671	–0.085
18	0.155	0.146	0.009
19	2.347	2.553	–0.206
20	3.22	3.034	0.188

Model D. It is well known that the variation in the observed biological activity is influenced by combination of different types of physicochemical properties. Therefore generation of QSAR models by clubbing together the descriptors belonging to different categories and allowing GFA to choose a proper, combination of descriptors, can have best internal and external predictivity along with proper balance of other statistical parameters. Model D was generated by using 32 descriptors. The GFA has indicated dominant role of Dipole–Z, AlogP, NCOSV, COSV and Apol descriptors, as these are frequently used in the generation of QSAR models. Best five equations were selected and are shown in the Table 5. Eq. (3) was chosen as representative of Model D, which has more

proper balance of all statistical terms than the rest of the models i.e., low LOF, higher r^2_{cv}, r^2, and F values along with proper external predictivity. The incorporation of all the descriptors resulted in an increase in the internal consistency of the molecules considered for generation of models. Hence, Eq. (3) of Model D was also selected to explain the variation in the inhibitory activity of tetrahydroisoindoles. The observed and predicted biological activities of training and test set molecules are given in Table 6 and 7 respectively.

Table 7. Observed and predicted biological activities of test set with Model D, Table 4

Molecule	Observed pIC_{50}	Predicted pIC_{50}	Residual
21	0.301	0.496	– 0.195
22	2.959	2.065	+ 0.894
23	2.796	2.435	+ 0.361
24	1.448	2.045	– 0.597
25	2.000	1.624	+ 0.376
26	1.542	1.694	– 0.152
27	2.000	2.450	– 0.450

3.2 Randomization Tests

To determine the model's reliability and significance, the randomization procedure was performed at 95 % (19 trials) and 98 % (49 trials) confidence level. The randomization was done by repeatedly permuting the dependent variable set. If the score of the original QSAR model proved better than those from the permuted data sets, the model would be considered statistically significant better than those obtained from the permuted data. The results of 19 and 49 trials of randomization tests are shown in the Table 8. The correlation coefficient r^2 for the nonrandom QSAR model was 0.772, significantly better than those obtained form randomized data. None of the permuted sets produced an r^2 comparable with 0.772; hence, the value obtained for the original GFA model is significant.

Table 8. Results of Randomization Tests

Confidence Level	Trials	$r^2_{nonrandom}$	r^2_{random} (Mean)	SD [a]	SD [b]	$r^2 <$ [c]	$r^2 >$ [d]
95 %	19	0.773	0.165	3.502	0.165	19	0
98 %	49	0.773	0.139	3.599	0.140	49	0

[a] Number of standard deviations of the mean value of r^2 of all random trials to the non–random r^2 value
[b] Standard deviation of the r^2 values of all random trials from the mean value of r^2
[c] number of r^2 values from random trials that are less than the r^2 value for the non–random trial
[d] number of r^2 values from random trials that are greater than the r^2 value for the non–random trial

3.3 Discussion

The Cerius2 QSAR module provides different descriptors divided into categories like thermodynamic, conformational, electronic, spatial, structural and receptor. Among these, some descriptors constitute a default set. Using this default set we obtained a reasonably well predictable model (Model A) with cross–validated r^2 (r^2_{cv}) 0.510. Therefore, in order to optimize the internal

and external predictivity the default descriptor set was extended in three different ways by including (*a*) thermodynamic, (*b*) MSA, and (*c*) all thirty two (2D and 3D) descriptors available in the Cerius2 QSAR module to generate different models by using GFA. With these additions the models were greatly improved in terms of internal and external consistency.

3.3.1 Interpretation of models

The frequent occurrence of AlogP and APol in Model A, B, and C clearly underlines the importance of thermodynamic and electronic descriptors for inhibition of COX–2 enzyme for the current series of molecules. AlogP is thermodynamic descriptor and represent hydrophobicity. By looking at the structure of the molecules it is evident that they are highly lipophilic, hence the appearance of AlogP is not a surprising one. AlogP is correlated positively, as COX–2 active site is hydrophobic in nature, and molecules with proper lipophilicity and bulkiness as that of most active compound may have same or enhanced enzyme inhibition property. It appears that an increase in the bulkiness of functional group(s) on aromatic ring(s) may lead to less active compound, as bulkiness may disorient the aromatic ring away from favorable interactions with active site residues. For example, compound **18** having a sulfonyl group, bulkier than most active compound, is less active because it may not be accommodated in the active site properly to have favorable interactions. APol is an electronic descriptor related to distribution of mass and is also proportional to the number of valence electrons in a molecule, as well as how tightly they are bound to their nuclei. Its presence is important because this term is unique for this class due to presence of nitrogen (in most of the molecules) or sulfur (compound **10**) in the polycyclic fused pyrrole or thiophene ring. The APol term in the QSAR models supports the biological activity that molecules containing unsubstituted nitrogen in the ring are more active than the corresponding substituted analogues. This implicates the possibility of charge transfer and electronic interactions between ligand and enzyme responsible for activity.

Model A. Along with AlogP and Apol, Model A contains descriptors like Hbond donor (structural) and RadOfGyration (spatial). Hbond donor is positively correlated to biological activity, it indicates that presence of Hbond donor group(s) in the molecule, allow it to retain the activity, in other words the –N– of pyrrole which is the only hydrogen donor group should be unsubstituted for better activity against COX–2 or even if substituted should contain hydrogen bond donor groups. For example, compounds **3** and **4** that contain substitution on pyrrole –N– are less potent than the unsubstituted analogues but are more potent than the non–hydrogen bond donor substituted compounds (compounds that are not included in the study as they are totally inactive to be considered for the generation of models). RadOfGyration is a spatial descriptor measuring the rigidity of the molecules needed for activity.

Model B. The model contains the descriptors from Model A but lack a spatial descriptor. Statistically, a combination of default and thermodynamic descriptors yielded improved model as

indicated by increase in the internal consistency, F value and lower LOF value. The importance of descriptors appeared in the equations are same as explained above.

Model C. The model was obtained by incorporating shape descriptors considering the fact that a variation in the topology/shape/structure of molecule will yield fluctuation in the biological activity for a set of molecules belonging to same class. Variable usage graph hints that shape descriptors such as COSV, NCOSV, and Vm play an important role in the construction of QSAR models along with thermodynamic and electronic. The appearance of COSV in the equation clearly indicates that the variation in the structure plays an important role. This model is characterized by low LOF, higher F value, and slightly improved internal consistency than Model A. Hence, the combination of MSA and default descriptors is significant.

Model D. In search of combination of descriptors that can give meaningful QSAR, models the default descriptors were combined with thermodynamic and shape descriptors separately. The obtained models were improved statistically compared to those constructed only with default descriptors. This forced to combine all the descriptors of different classes and to generate a model.

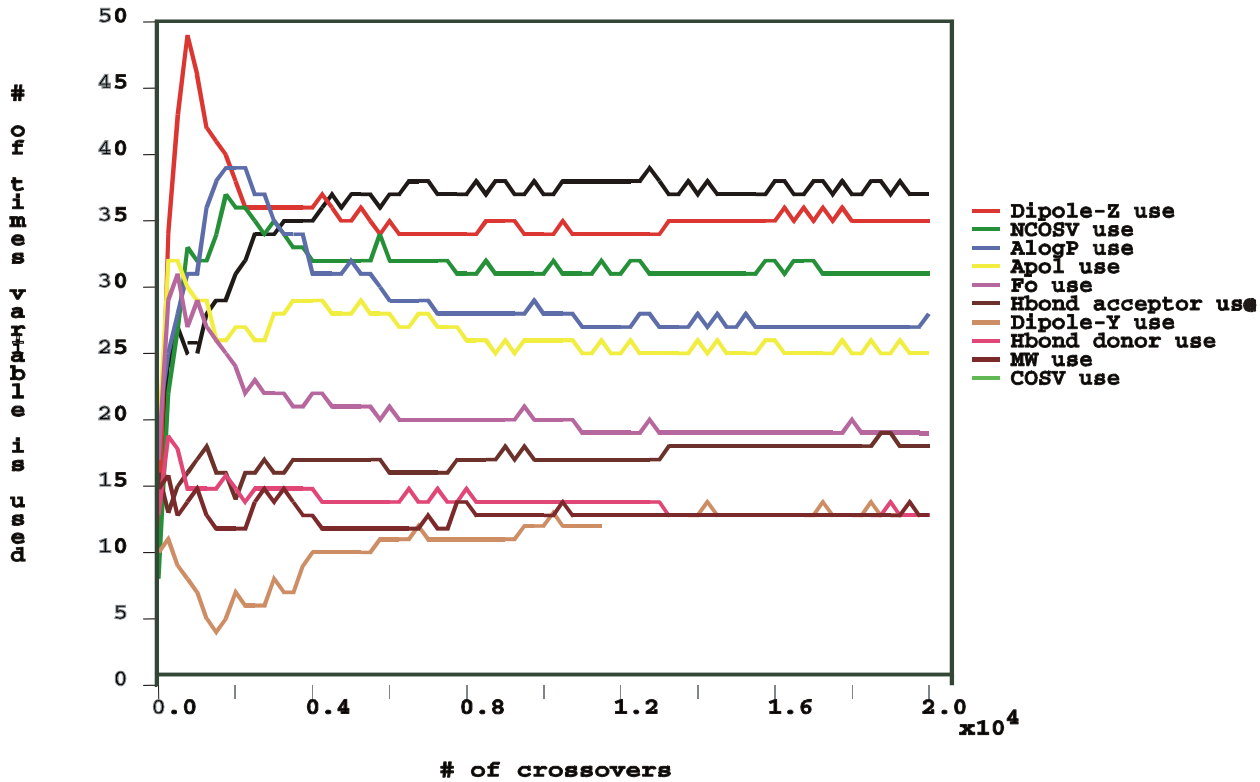

Figure 3. Variable usage graph.

The variable usage graph (Figure 3) has shown a different phenomenon in the generation of QSAR equations, along with AlogP and APol, which were used extensively in the earlier models, *i.e.*, they were accompanied by Dipole–Z, NCOSV and COSV for the generation of the current model. In all aspects, the model has improved statistical terms except r^2_{pred}, which is slightly

smaller than in earlier models. Higher r^2_{cv}, r^2, F, a very low LOF values and a proper r^2_{pred} clearly indicates that Model D is superior among all other models. Hence, we chose this model as the equation, to explain the observed biological activity for new class of COX–2 enzyme inhibitors. Graph of observed and predicted biological activities of training and test set are shown in the Figure 4 and 5 respectively.

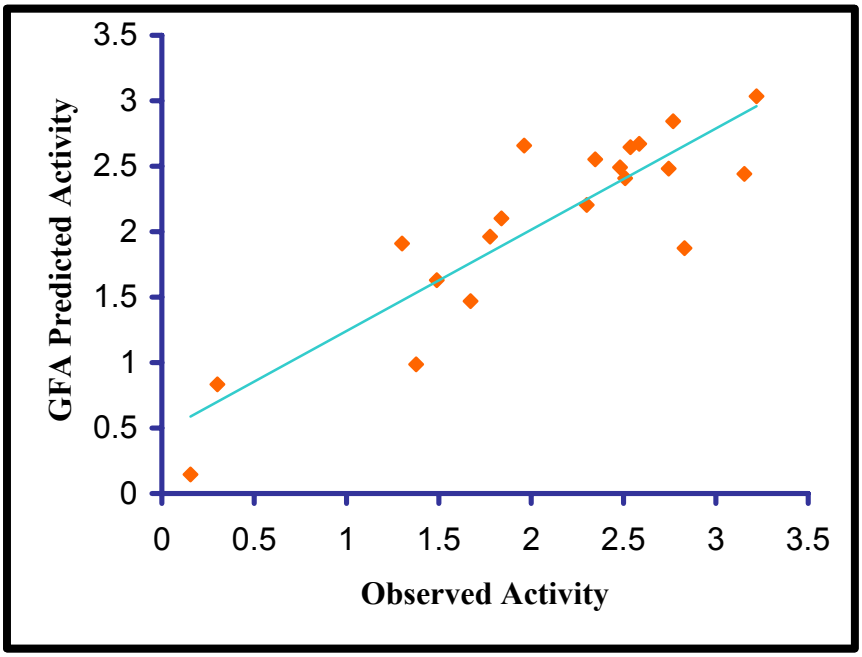

Figure 4. Observed and GFA predicted biological activities of training set (Model D, Table 4).

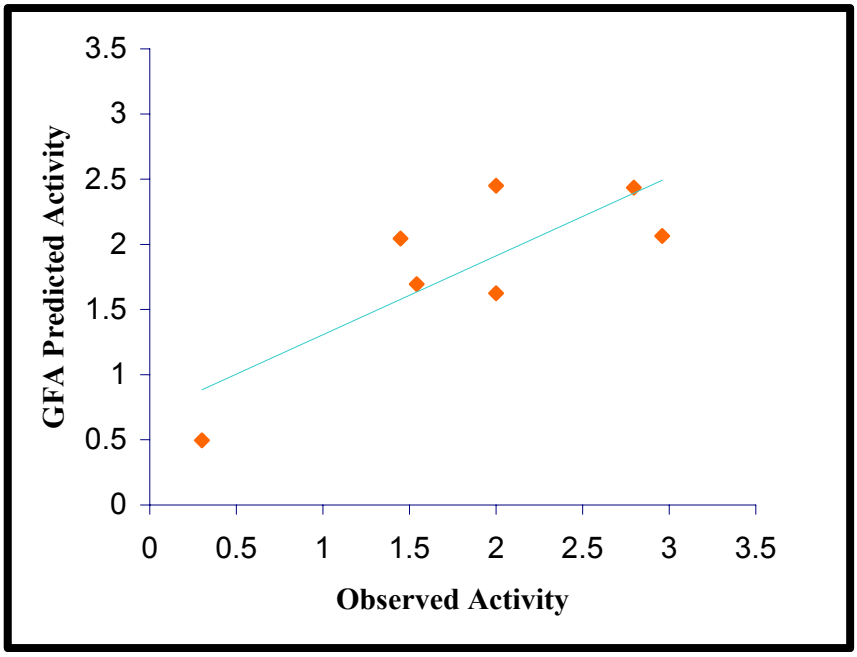

Figure 5. Observed and GFA predicted biological activities of test set (Model D, Table 4).

3.3.2 Interpretation of the descriptors in the selected QSAR equation

The observed COX–2 enzyme inhibition activity for 1,3–diaryltetrahydroisoindole derivatives is influenced by descriptors COSV, Dipole–Z, and PMI–Z. The descriptors COSV and Dipole–Z were positively correlated and PMI–Z negatively correlated.

COSV. It is the common volume between shape reference and the other analogues. Because the shape reference molecule is the one with highest biological activity and COSV is positively correlated, molecules that are structurally/conformationally similar to the most active molecule are expected to exhibit higher activity. The presence of COSV also indicates the importance of conformational rigidity of the two aromatic rings attached to central pyrrole nucleus of the molecules. Guillaume *et al*., while explaining SAR in the original paper, described that the attachment of polycyclic rings increases the bulkiness (steric), and an increase in hydrophobic character of the inhibitors will enhance the enzyme inhibition property [5]. This may be due to the attachment of polycyclic rings to pyrrole nucleus additionally which may give proper rigidity to it and in turn allowing the two aromatic rings to have proper conformation, so to occupy a larger area in the active site of enzyme.

Dipole–Z. It is an electronic descriptor and indicates the strength and orientation behavior of polarizable functional group(s) of a molecule in electrostatic field. The active analogue (compound **20**) of the current series contains two fluoro groups on the aromatic rings attached to pyrrole nucleus. One of the aromatic rings bearing fluoro functionality is oriented towards Dipole–Z component, *i.e*. perpendicular to pyrrole nucleus. Therefore, the presence of small polarizable groups oriented at Z component may allow the molecule to retain activity as that of active analogue. Increase in the bulkiness of polarizable group may yield slightly less active compounds, such as **8**. Thus the dipole interactions are important for COX–2 enzyme inhibition.

PMI–Z. PMI–Z is a spatial descriptor and indicates the orientation and conformational rigidity of the molecule. Thus the orientation of the aromatic ring bearing small polarizable groups along Z–axis is important for the enzyme inhibition.

The crystal structures of both COX–1 and COX–2 are available and active sites of both isoforms have been explored. It is well established that the active site of COX–2 is flexible and offers various chemical moieties to act either as substrates or inhibitors [6]. The molecules under study are potent COX–2 inhibitors and characterized by lacking primary requisites present in various tricyclic classes of newly developed COX–2 inhibitors. Guillaume *et al*., while explaining the SAR mentioned that, when functional groups thought to induce COX–2 selectivity for tricyclic inhibitors were retained, the molecules lost COX–2 selectivity (compound **18**) [5]. Hence, they concluded that the binding mode for this diverse class in COX–2 active site might be different than the tricyclic class of COX–2 inhibitors. Therefore, at this stage it would be appropriate to compare the descriptors appeared in the model, selected for explaining the SAR with the protein topology.

3.3.3 Hypothetical mechanism of ligand–enzyme interaction

The final equation (Model D, Table 4) contains COSV and Dipole–Z as positively correlated terms and PMI–Z correlated negatively.

COSV. The common overlap steric volume would be significant in terms of occupation at the enzyme–binding site, as it represents the volume available for binding. The COSV is positively correlated and as the shape reference (compound **20**) is bulkier it indicates that the active site of COX–2 enzyme is large. The volume of the COX–2 active site is approximately 20–25% larger than that of COX–1, because the presence of smaller amino acid in position 523 in COX–2 (valine in COX–2; isoleucine in COX–1) induces a conformational change, thereby forming an additional hydrophobic secondary internal pocket protruding off the primary binding site which is absent in COX–1 [23,24]. Consequently, the total volume of COX–2 primary binding site and its associated secondary pocket (394 $Å^3$) is about 20–25% larger than that of COX–1 binding site (316 $Å^3$). Though the molecules lack traditional requisite functional groups, but probably due to their bulkiness (331.70 $Å^3$ for the most active) are capable of occupying larger area (84.18% by most active molecule) in the active site and making proper interactions with active site residues hence are active. Thus positively correlated COSV in our equation is justified.

Dipole–Z. The appearance of positively correlated Dipole–Z indicates the presence of electronic and π–π interactions between the molecule and active site residues. These kinds of interactions are common in COX–2 enzyme inhibitors, particularly in case of tricyclic inhibitors. Because the primary and secondary active sites of COX–2 enzyme are lined by amino acid derivatives that are capable of having electrostatic interactions with appropriate functional groups present in the inhibitors. Ex: (*a*) His90, Gln192, and Tyr355 (control the access of ligands into the secondary pocket by hydrogen bonding network) [25], (*b*) Tyr385, Ser530, Arg120 and recently Arg513 in the primary active site [26]. Recent molecular modeling studies reveal that the water molecules present near the mouth of the active site play major role in the remodeling of the hydrogen–bonding network involving Arg120 and Glu524 which is necessary for time dependent inhibition of enzyme by the inhibitors. In the present study the contribution of dipole moment is mainly from aromatic rings and its substituents like fluoro and –N– of pyrrole nucleus. The SAR of molecules under study reveals that molecules with an unsubstituted pyrrole nitrogen and with fluoro substituted aromatic rings have retained the enzyme inhibition profile because it may be possible that the –H– of pyrrole nitrogen may involve in the hydrogen bond formation with the water molecules or the functional groups present on the aromatic rings may have electrostatic interactions with the active site residues as mentioned above.

PMI–Z. PMI indicates orientation and conformational rigidity of the molecule and its value depends on the total mass distribution within the molecule. In the tricyclic class of COX–2 inhibitors, central heterocyclic core if it is substituted by an additional substituent or if it has an

additional fused five or six–member ring may orient more favorably the ligand within the COX–2 binding site to enhance COX–2 selectivity [27]. Therefore, for the molecules under study, constitution of central pyrrole core by bicyclic ring system may be needed as it may provide rigidity to pyrrole nucleus and may facilitate rotatory motion of the molecule around the principle axis so as to orient the each aromatic ring in a proper direction particularly one ring bearing small polarizable group, towards the Z component. This kind of orientation may provide molecule to attain a proper shape or orientation or conformation, which fit best in the active site of COX–2 enzyme, retaining necessary interactions with active site residues.

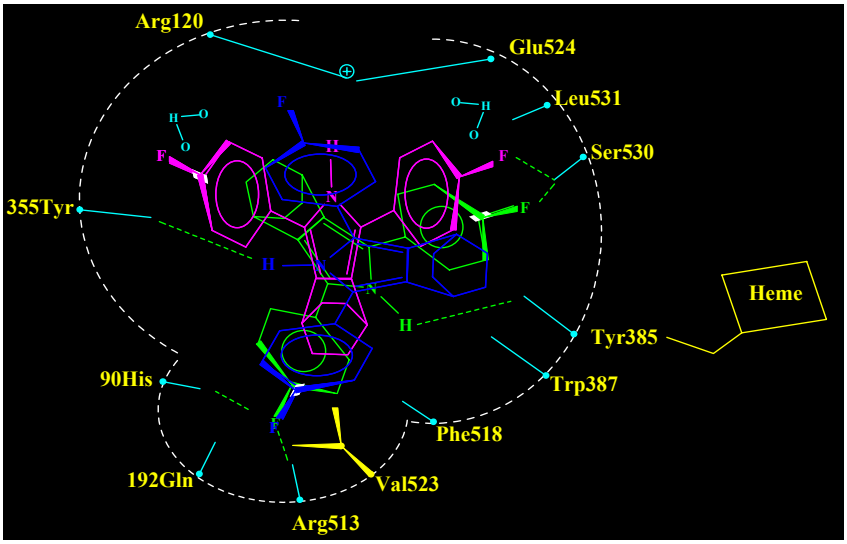

Figure 6. Most possible binding modes of the active molecule.

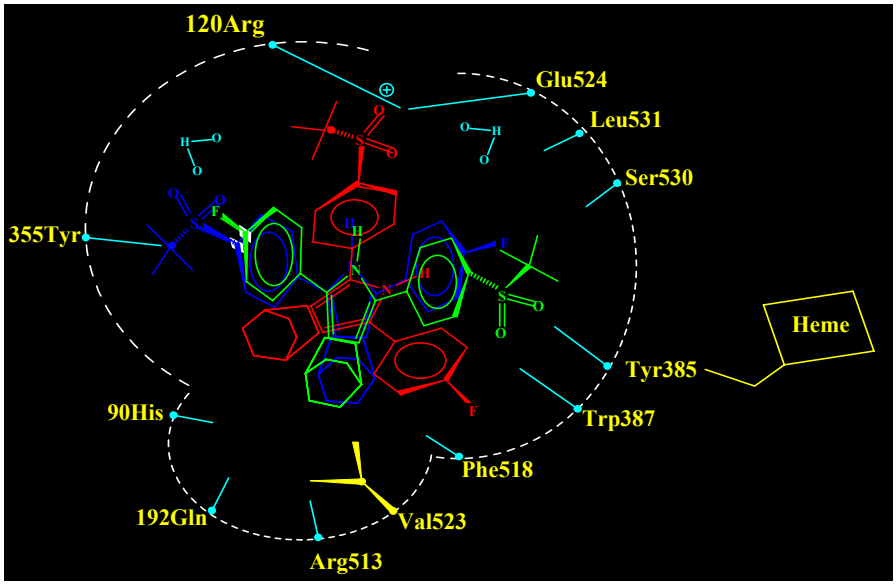

Figure 7. Most possible binding modes of the inactive molecule.

Though AlogP not appeared in the final equation but its appearance in three models out of four (Table 4) clearly indicates that the active site of the enzyme in which these molecules bind, may be hydrophobic and it is well established in the literature [24].

Therefore, broadly it can be concluded that, QSAR models developed from different combinations of the descriptors indicate that the inhibition of COX–2 enzyme may be non–covalent in nature and depends upon shape (steric), electronic, and conformational (spatial or orientation) properties of the molecules. Most probable orientations of active (compound **20**) and inactive (compound **18**) molecules in the COX–2 active sites are given in the Figure 6 and 7 respectively.

3.3.4 Comparison of model with the earlier QSAR studies

The discovery of COX–2 enzyme has led to the development of different classes of COX–2 inhibitors by various research groups. Then onwards the COX–2 enzyme has become a fruitful target for drug design. Several molecular modeling studies have been performed on COX–2 inhibitors, but only a few QSAR studies on this class have appeared in the literature. The methods employed include CoMFA, CoMSIA, ANN and classical QSAR and recently Liu *et al*. reported a QSAR of COX–2 inhibitors with Molecular Electronegativity Distance Vector as descriptors along with combination of Genetic Algorithm and MLR method [28–36]. The CoMFA and CoMSIA for tricyclic COX–2 inhibitors reveal that the COX–2 site is hydrophobic and its inhibition is driven by optimum hydrophobicity and steric interactions. Small polarizable functional groups are necessary to occupy the secondary pocket for COX–2 inhibition. All the QSAR studies appeared in literature were performed on vicinal diaryl compounds. The descriptors appeared in the final equation and other models of present study are complementary with the topology of the enzyme active site and hence, are consistent with the earlier molecular modeling and QSAR studies.

4 CONCLUSIONS

Series of 1,3–diaryl–4,5,6,7–terahydro–2, 4–isoindole derivatives are reported as potent COX–2 inhibitors with very good antiinflammatory activity. 1,3–diaryl substitution on the central polycyclic ring system and absence of a sulfonyl moiety on the phenyl ring are two distinctive structural features that distinguishes this new chemical series from the COX–2 inhibitors known till date. QSAR analysis was performed using robust statistical technique GFA, coupled with the use of combinations of different classes of descriptors. The generated models were analyzed for their statistical significance. The models were also validated for their external prediction power.

GFA handled the physico–chemical descriptors effectively in the generations of QSAR models with significant statistical terms including external predictivity. For the current series of molecules the descriptors COSV, Dipole–Z, and PMI–Z appears to contribute significantly for the observed biological activity. The current QSAR analysis reveals that the inhibition of COX–2 enzyme by

these diverse set of molecules may be non covalent in nature and depends upon shape (steric), electronic and spatial (conformational) properties of the molecules. The selected model has good internal and external prediction power. Low values of correlation coefficient obtained from the randomized tests than the non–randomized tests clearly indicates the significance of the model generated by GFA. The descriptors appeared in the model are complementary to the COX–2 enzyme topology. An attempt has been made to develop a hypothetical mechanism of inhibitor and enzyme interaction. Due to bulkiness, the molecules may occupy larger COX–2 binding site, which is being same for tricyclic class of inhibitors but may have different interactions with the active site residues. The presence of small polarizable functional group may improve COX–2 inhibitory potency.

Although results obtained from different Models A to C are fairly significant in terms of statistical measurements but indicate that various descriptors might play a role in determining the COX–2 inhibition in different experimental conditions. Therefore, by averaging the results of multiple models, the utility of modeling study can be increased, rather than relying on an individual model.

Acknowledgment

The authors gratefully acknowledge support from the University Grants Commission (UGC), New Delhi, under its DSA and COSIST programs.

5 REFERENCES

[1] J. R. Vane, Inhibition of Prostaglandin Synthesis as a Mechanism of action for Aspirin–like Drugs, *Nature New Biol*. **1971**, *231*, 232–235.

[2] *a*) W. Xie, J. G. Chipman, D. L. Robertson, R. L. Erickson, and D. L.Simmons, Expression of a Mitogen–Responsive Gene Encoding Prostaglandin Synthesis is Regulated by mRNA Splicing, *Proc*. *Natl*. *Acad*. *Sci*. *U.S.A*. **1991**, *88*, 2692–2696; *b*) D. A. Kujubu, B. S Fletcher, B. C. Varnum, R. W. Lim, and H. R. Herschman, TIS 10, A Phorbol Ester Tumor Promoter–inducible mRNA from Swiss 3T3 Cells Encodes A Novel Prostaglandin Synthase / Cyclooxygenase Homologue, *J*. *Biol*. *Chem*. **1991**, *266*, 12866–12872.

[3] J. J. Talley, Selective Inhibitors of Cyclooxygenase–2 (COX–2), *Prog*. *Med*. *Chem*. **1999**, *36*, 201–234.

[4] W. Kiefer, and G. Dannhardt, Cyclooxygenase Inhibitors – Current Status and Future Prospects, *Eur*. *J*. *Med*. *Chem*. **2001**, *36*, 109–126.

[5] P. Bernard, T. Charles, P. Philippe, B. Jacqueline, and De. N. Guillaume, 1, 3–Diaryl–4, 5, 6, 7–tetrahydro–2*H*–isoindole Derivatives. A New Series of Potent and Selective COX–2 Inhibitors in Which a Sulfonyl Group is Not a Structural Requisite, *J*. *Med*. *Chem*. **2000**, *43*, 4582–4593.

[6] C. Luong, A. Miller, J. Barnett, J. Chow, C. Ramesha, and M. F. Browner, Flexibility of the NSAID Binding Site in the Structure of Human Cyclooxygenase–2, *Nature*.*Struct*. *Biol*. **1996**, *3*, 927–933.

[7] V. M. Gokhale, and V. M. Kulkarni, Understanding the Antifungal Activity of Terbinafine Analogues Using Quantitative Structure–Activity Relationship (QSAR) models, *Bioorg*. *Med*. *Chem*. **2000**, *8*, 2487–2499.

[8] R. G. Karki, and V. M. Kulkarni, Three–Dimensional Quantitative Structure Activity Relationship (3D–QSAR) of 3–Aryloxazolidin–2–one Antibacterials, *Bioorg*. *Med*. *Chem*. **2001**, *9*, 3153–3160.

[9] M. T. Makhija, and Kulkarni V. M. QSAR of HIV–1 Integrase Inhibitors by Genetic Function Approximation Method, *Bioorg*. *Med*. *Chem*. **2002**, *10*, 1483–1497.

[10] Unpublished results. Part of a Ph. D. Thesis submitted to the University of Mumbai, 2002.

[11] P. S. Kharkar, B. Desai, B. Varu, R. Loriya, Y. Naliyapara, H. Gaveria, A. Shah and V. M. Kulkarni, Three–Dimensional Quantitative Structure Activity Relationship Of 1,4–Dihydropyridines as Antitubercular Agents, *J*.

Med. *Chem*. **2002**, ***45***, 4858–4867.
[12] D. Rogers, G/SPLINES: A Hybrid of Friedman's Multivariate Adaptive Regression Splines (MARS) Algorithm with Holland's Genetic Algorithm, *Proceedings of the Fourth International Conference on Genetic Algorithms*, San Diego, July 1991.
[13] D. Rogers, and A. J. Hopfinger, Applications of Genetic Function Approximation to Quantitative Structure–Activity Relationships and Quantitative Structure–property Relationships, *J. Chem*. *Inf*. *Comput*. *Sci*. **1994**, *34*, 854.
[14] P. Venkatarangan and A. J. Hopfinger, Prediction of Ligand–Receptor Binding Thermodynamics by Free Energy Force Field 3D–QSAR Analysis: Application to a Set of Glucose Analogue Inhibitors of Glycogen Phosphorylase, *J*. *Med*. *Chem*. **1999**, *4*2, 2169–2179.
[15] J. S. Tokarski, and A. J. Hopfinger, Prediction of Ligand–Receptor Binding Thermodynamics by Free Energy Force Field 3D–QSAR Analysis: Application to a Set of Peptidometic Renin Inhibitors, *J. Chem*. *Inf*. *Comput*. *Sci*. **1997**, *37*, 792–811.
[16] M. Hann, and D. Rogers, Receptor Surface Models 2. Application to QSAR Studies, *J. Med*. *Chem*. **1995**, *38*, 2091–2102.
[17] Y. Fan, L. M. Shi, K. W. Kohn, Y. Pommier, and J. N. Weinstein, Quantitative Structure–Antitumor Activity Relationship of Camptothecin Analogues: Cluster Analysis and Genetic Algorithm Based Studies, *J. Med*. *Chem*. **2001**, *44*, 3254–3263.
[18] Cerius2 version 3.5 is available from Molecular Simulations Inc., 9685, Scranton Road; San Diego, CA. USA 92121.
[19] A. K. Rappe, and W. A Goddard, III Charge Equilibration for Molecular Dynamics Simulations, *J. Phy*. *Chem*. **1991**, *95*, 3358–3363.
[20] A. J. Hopfinger, A Quantitative Structure Activity Relationship. Investigation of Dihydrofolate Reductase Inhibition by Baker Triazines Based Upon Molecular Shape Analysis, *J. Am*. *Chem*. *Soc*. **1980**, *102*, 7196–7206.
[21] C. L Waller, T. I Opera, A. Giolitti, and G. R. Marshall, Three–Dimensional QSAR of Human Immunodeficiency Virus (1) Protease inhibitors. 1. A CoMFA Study Employing Experimentally Determined Alignment Rules, *J. Med*. *Chem*. **1993**, *36*, 4152–4160.
[22] R. D. III. Cramer, J. D Bunce, and D. E. Patterson, Cross–validation, Bootstrapping and partial Least Squares Compared With Multiple Regressions in Conventional QSAR Studies, *Quant*. *Struct*. *Act*. *Relat*. **1988**, *7*, 18–25.
[23] J. K Gierse, J. J. McDonald, S. D. Hauser, S. H. Rangwala, C. M. Koboldt, and K. Seibert, A Single Amino Acid Difference Between Cyclooxygense–1 (COX–1) and –2 (COX–2) Reverses the Selectivity of COX–2 Specific Inhibitors, *J. Biol*. *Chem*. **1996**, *271*, 15810–15814.
[24] R. G. Kurumbail, A. M. Stevens, J. K. Gierse, J. J. McDonald, R. A. Stegeman, J. Y. Pak, D. Gildehaus, J. M. Miayshiro, T. D. Penning, K. Seibert, P. C. Isakson, and W. C. Stallings, Structural Basis for Selective Inhibition of Cycooxygenase–2 by Antiinflammatory Agents, *Nature*. **1996**, *384*, 644–648.
[25] O. Llorens, J. J. Perez, A. Palomer, and D. Mauleon, Structural Basis of The Dynamic Mechanism of Ligand Binding to Cyclooxygenase, *Bioorg*. *Med*. *Chem*. *Lett*. **1999**, *9*, 2779–2784.
[26] A. G Habbeb, P. N. Praveen Rao, and E. E. Knaus, Design and Synthesis of Celecoxib and Rofecoxib Analogues as Selective Cyclooxygenase–2 (COX–2) Inhibitors: Replacement of Sulfonamide and Methanesulfonyl Pharmacophore by an Azido Bioisostere, *J. Med*. *Chem*. **2001**, *44*, 3039–3042.
[27] J. S. Carter, D. J. Rogier, M. J. Graneto, K. Seibert, C. M. Koboldt, Y. Zhang, and J. J. Talley, Design and Synthesis of Sulfonyl Substituted 4, 5–Diarylthiazoles as Selective Cyclooxygenase–2 inhibitors, *Bioorg*. *Med*. *Chem*. *Lett*. **1999**, *9*, 1167–1170.
[28] R. Kumar, and P. Singh, Diarylspiro[2.4]Heptenes as Selective Cyclooxygenase–2 Inhibitors: A QuantitativeStructure–Activity Relationship Analysis, *Indian* J. *Che*m. *B* **199**7, *3*6, 1164–1168.
[29] P. Singh and R. Kumar, Novel Inhibitors of Cyclooxygenase–2: The Sulfones and Sulfonamides of 1,2–Diaryl–4,5–Difluorobenzene. Analysis of Quantitative Structure–Activity Relationship, J. *Enzyme*. *Inhi*b. **199**8, *1*3, 409–417.
[30] P. Singh and R. Kumar, 1,2–Diarylimidazoles as Inhibitors of Cyclooxygenase–2: A Quantitative Structure–Activity Relationship Study, J. *Enzyme Inhi*b. **199**9, *14*, 277–288.
[31] C. Marot, P. Chavatte, and D. Lesieur, Comparative Molecular Field Analysis Of Selective Cyclooxygenase–2 (COX–2) Inhibitors, *Quan*t. *Struc*t.*–Ac*t. *Rela*t. **200**0, *19*, 127–134.
[32] G. R. Desiraju, B. Gopalakrishnan, R. K. R. Jetti, D. Raveendra, J. A. R. P. Sarma, and H. S. Subramanya, Three–Dimensional Quantitative Structural Activity Relationship (3D–QSAR) Studies of Some 1,5–Diarylpyrazoles: Analogue Based Design of Selective Cyclooxygenase–2 Inhibitors, *Molecules* **200**0, 5, 945–955.
[33] P. Chavatte, S. Yous, C. Marot, N. Baurin, and D. Lesieur, Three–Dimensional Quantitative Structure– Activity Relationships of Cyclo–Oxygenase–2 (COX–2) Inhibitors: A Comparative Molecular Field Analysis, J. *Me*d. *Che*m. **200**1, *4*4, 3223–3230.
[34] S.–S. Liu, H.–L. Liu, Y.–Y. Shi, and L.–S. Wang, QSAR of Cyclooxygenase–2 (COX–2) Inhibition by

2,3–Diarylcyclopentenones Based on MEDV–13, *Internet Electron. J. Mol. Des.* **2002**, *1*, 310–318, http://www.biochempress.com.

[35] H. Liu, X. Huang, J. Shen, X. Luo, M. Li, B. Xiong, G. Chen, J. Shen, Y. Yang, H. Jiang, and K. Chen, Inhibitory Mode of 1,5–Diarylpyrazole Derivatives against Cyclooxygenase–2 and Cyclo–oxygenase–1: Molecular Docking and 3D QSAR Analyses. *J. Med. Chem.* **2002**, *45*, 4816–4827.

[36] G. R. Desiraju, B. Gopalakrishnan, R. K. R. Jetti, A. Nagaraju, D. Raveendra, J. A. R. P. Sarma, M. E. Sobhia, and R. Thilagavathi, Computer–Aided Design of Selective COX–2 Inhibitors: Comparative Molecular Field Analysis, Comparative Molecular Similarity Indices Analysis, and Docking Studies of Some 1,2–Diarylimidazole Derivatives, *J. Med. Chem.* **2002**, *45*, 4847–4857.

Biographies

Vithal M. Kulkarni is Professor of Medicinal Chemistry and Head of Pharmaceutical Technology and Pharmacy Division, Mumbai University, Institute of Chemical Technology. He was postdoctoral visiting fellow in T. I. F. R. (1974–76) Mumbai and at Borstel Research Institute, Germany (1979–1981). His areas of research specialization include (1) Chemotherapy of tropical, viral and fungal diseases (2) Computer Aided Drug Design. (3) Synthesis of novel drugs and intermediates. He has presented / published numerous papers in reputed national and international conferences and journals. He is research investigator and consultant for several pharmaceutical industries. He is recipient of Prof. (late) M. L. Khorana memorial Lecture Award, Eminent Pharmacist Award of Indian Pharmaceutical Association and Best Teacher Award of University of Mumbai.

Anand V. Raichurkar is a Research Fellow and is pursuing doctoral studies under the guidance of Prof. V. M. Kulkarni. He is M. Pharm from Rajiv Gandhi University of Health Sciences, Bangalore. His research interests are (1) Computer Aided Drug Design. (2) Synthesis of New Chemical Entities as antibacterials, antiinflammatory and anticancer agents. He has presented / published research papers in national and international conferences and journals.